Cell. Mol. Life Sci. 65 (2008) 2763 – 2775
1420-682X/08/172763-13
DOI 10.1007/s00018-008-8329-2

Cellular and Molecular Life Sciences

Research Article

Selenocystine induces apoptosis of A375 human melanoma cells by activating ROS-mediated mitochondrial pathway and p53 phosphorylation

T. Chen and Y. S. Wong*

Department of Biology, Ma Lin Building, Science Centre, The Chinese University of Hong Kong, Shatin, Hong Kong SAR (China), Fax: +852 2603 5745, e-mail: yumshingwong@cuhk.edu.hk

Received 12 June 2008, received after revision 02 July 2008, accepted 08 July 2008
Online First 26 July 2008

Abstract. Selenocystine (SeC), a naturally occurring selenoamino acid, has been shown to be a novel compound with broad-spectrum anticancer activity. In this study, we showed that SeC triggered time- and dose-dependent apoptosis in A375 human melanoma cells by activating the mitochondria-mediated and death receptor-mediated apoptosis pathways. Pretreatment of cells with a general caspase inhibitor z-VAD-fmk significantly prevented SeC-induced apoptosis. A375 cells exposed to SeC showed an increase in levels of total p53 and phosphorylated p53 (serine-15). Silencing of p53 expression with RNA interference significantly suppressed SeC-induced p53 phosphorylation, caspase activation and apoptotic cell death. Moreover, generation of reactive oxygen species and subsequent induction of DNA strand breaks were found to be upstream mediators of p53 activation induced by SeC. In a nude mice xenograft experiment, SeC significantly inhibited the tumor growth of A375 cells via induction of apoptosis. Taken together, these results suggest the potential applications of SeC in cancer chemoprevention.

Keywords. Selenium, selenocystine, melanoma, apoptosis, mitochondria, p53, reactive oxygen species.

Introduction

Malignant melanoma is a rapidly spreading skin tumor with a very high invasive capacity and growing incidence [1]. Due to the high metastatic potentials and resistance towards chemotherapy, radiotherapy, and immunotherapy [2], the management of melanoma represents one of the most challenging problems in clinical oncology [3]. Although great improvement in survival rate of disseminated melanoma by using the contemporary therapeutic strategies, severe side effects, such as thrombocytopenia, neutropenia and anemia are unavoidable. Therefore, the search for new agents capable of selectively killing melanoma cells constitutes an urgent priority.

Apoptosis or programmed cell death plays a major role in the development, homeostasis, and prevention of cancer. Induction of apoptosis has been considered the major cytotoxic mechanism of anticancer therapies. Generally, apoptosis may occur via the mitochondrial (intrinsic) pathway [4] and the death receptor (extrinsic) pathway [5]. The mitochondrial pathway is mediated by Bcl-2 family proteins, which disrupt the mitochondria membrane potential, resulting in release of apoptogenic factors from the mitochondria to the cytosol, such as cytochrome c, Smac/Diablo and apoptosis-inducing factor (AIF). Cyto-

* Corresponding author.

chrome c in cytosol would form an apoptosome with apoptosis activating factor 1 and caspase-9, and then activate the downstream apoptotic signals [4, 6]. The extrinsic pathway is triggered through the formation of death inducing signaling complex, which subsequently activates initiator caspase-8 and then cleaves executioner caspases [5, 7]. At present, it is recognized that resistance to apoptosis is a critical factor in tumor progression and malignancy. Studies showed that the major mechanism accounting for drug resistance in melanoma is the dysregulation of apoptosis through over-expression of pro-survival proteins and down-regulation of pro-apoptotic proteins [8]. The understanding of the mechanisms by which melanoma cells escape from apoptosis would be beneficial in the design and development of novel chemopreventive agents.

Selenium (Se) is a mineral trace element of fundamental importance to humans and animals [9]. The role of selenocompounds as potential cancer chemopreventive and chemotherapeutic agents has been supported by epidemiological, preclinical and clinical studies [10, 11]. Mechanistic studies indicated that cell apoptosis was one of the most critical mechanisms for anticancer action of Se [12]. Experimental studies have found that dietary supplementation of selenomethionine and high-Se soy protein reduced metastasis of melanoma cells in mice [13, 14]. Recently, selenomethionine was also found to be able to protect human skin cells from ultraviolet radiation-induced p53 transactivation [15]. However, the mechanism for the anticancer activity of Se against melanoma was never explored.

Selenocystine (SeC), a nutritionally available selenoamino acid, exhibits potential applications in chemotherapy. In our previous works, SeC was identified as a novel agent with higher antitumor activity than selenomethionine, Se-methyl-seleno-cysteine, selenite and selenate [16]. SeC showed novel antiproliferative effects on A375 human melanoma cells via induction of apoptosis in association with reactive oxygen species (ROS) generation. Despite this potency, SeC showed much lower cytotoxicity toward the HS68 human fibroblasts. The aim of this study was to investigate the roles of caspases, mitochondria, ROS and p53, and their crosstalk in SeC-induced apoptosis pathways. The results showed that SeC exhibited *in vitro* and *in vivo* inhibitory effects on A375 melanoma cells and triggered apoptosis by activating the ROS-mediated mitochondrial pathway and p53 phosphorylation.

Materials and methods

Materials. Selenocystine, propidium iodide (PI), solid JC-1, 4',6-Diamidino-2-phenyindole (DAPI), 2′,7′-dichlorofluorescein diacetate (DCF-DA), pifithrin-α and bicinchoninic acid kit for protein determination were purchased from Sigma. Reagent kit for single cell gel electrophoresis assay (Comet Assay) was purchased from Trevigen. The mitochondrial dye mitotracker red (CM-H_2Ros) was obtained from Molecular Probes. All of the antibodies used in this study and p53 small interfering RNAs (siRNA) were purchased from Cell Signaling Technology (Beverly, MA). The general caspase inhibitor (z-VAD-fmk) was purchased from Calbiochem. Se standard for ICP-AES detection was purchased from J. T. Baker. Eight chamber polystyrene vessels were obtained from Becton Dickinson Labware. The ultrapure water used for all experiments was supplied by a Milli-Q water purification system from Millipore.

Cell culture. A375 human melanoma cell line was obtained from American Type Culture Collection (ATCC, Manassas, VA) and maintained in DMEM medium supplemented with fetal bovine serum (10%), penicillin (100 units/ml) and streptomycin (50 units/ml) at 37°C in a humidified incubator with 5% CO_2 atmosphere.

MTT assay. Cell viability was determined by measuring the ability of cells to transform MTT to a purple formazan dye [16]. Cells were seeded in 96-well tissue culture plates at 2.0 x 10^3 cells/well for 24 h. The cells were then incubated with SeC at different concentrations for 24, 48 and 72 h. After incubation, 20 μl/well of MTT solution (5 mg/ml phosphate buffered saline) was added and incubated for 5 h. The medium was aspirated and replaced with 150 μl/well of acidic isopropanol (0.04 N HCl in isopropanol) to dissolve the formazan salt formed. The color intensity of the formazan solution, which reflects the cell growth condition, was measured at 570 nm using a microplate spectrophotometer (SpectroAmax™ 250).

Determination of Se. Se concentration was determined by ICP-AES method as previously described [17]. Briefly, collected cells were digested with 3 ml concentrated nitric acid and 1 ml H_2O_2 in an infrared rapid digestion system (Gerhardt) at 180°C for 1.5 h. The digested solution was reconstituted to 10 ml with Milli-Q H_2O and used for ICP-AES analysis.

Flow cytometric analysis. The cell cycle distribution was analyzed by flow cytometry as previously described [18]. Cells were trypsinized after treatments,

washed with PBS and fixed with 75% ethanol overnight at -20°C. The fixed cells were washed with PBS and stained with propidium iodide (PI) working solutions (1.21 mg/ml Tris, 700U/ml RNase, 50.1 μg/ml PI, pH 8.0) for 4 h in darkness. The stained cells were then subjected to an Epics XL-MCL flow cytometer (Beckman Coulter, Miami, FL). Cell cycle distribution was analyzed using MultiCycle software (Phoenix Flow Systems, San Diego, CA). The proportion of cells in G0/G1, S, G2/M phases was represented as DNA histograms. Apoptotic cells with hypodiploid DNA content were measured by quantifying the sub-G1 peak in the cell cycle pattern. For each experiment 10 000 events per sample were recorded.

TUNEL assay. Cells cultured in chamber slides were fixed with 3.7% formaldehyde for 10 min and permeabilized with 0.1% Triton X-100 in PBS. After that, cells were incubated with 100 μl/well TUNEL reaction mixture containing nucleotide mixture and terminal deoxynucleotidyl transferase (TdT) for 1 h at 37°C. The cells were then washed with PBS and examined by fluorescence microscopy (Nikon Eclipse 80i).

Evaluation of mitochondrial membrane potential ($\Delta\Psi m$). Cells cultured in six-well plates were trypsinized and resuspended in 0.5 ml of PBS buffer containing 10 μg/ml JC-1. After incubation for 10 min at 37°C in the incubator, cells were immediately centrifuged to remove the supernatant. Cell pellets were suspended in PBS and then analyzed by flow cytometry. The percentage of the green fluorescence from JC-1 monomers was used to represent the cells that lost $\Delta\Psi m$.

Single Cell Gel Electrophoresis (Comet Assay). Single-cell gel electrophoresis for detection of DNA damage was performed using the Comet assay reagent kit purchased from Trevigen according to the manufacturer's instructions. Briefly, cells treated with SeC were harvested by centrifugation at 1500 rpm (20°C, 5 min) and resuspended at 1×10^5 cells/ml in PBS. The cell suspension was mixed with melted LM agarose at a ratio of 1:10 (v/v). An aliquot (75 μl) of the mixture was immediately pipetted onto the slide (CometSlide™). After refrigeration for 30 min, the slide was immersed in prechilled lysis solution and left on ice for 60 min, followed by immersing in freshly prepared alkaline solution (300 mM NaOH, 1 mM EDTA, pH > 13) for 60 min on ice in darkness. After DNA unwinding, the slide was subjected to alkaline solution for electrophoresis in a Savant ps 250 system set at 300 mA and 1 volt/cm for 30 min. After electrophoresis, the slide was rinsed with distilled H_2O, fixed in 70% ethanol for 5 min and air-dried overnight. DNA was stained with SYBR Green I (Trevigen) and visualized under a fluorescence microscope (Nikon, Eclipse E-600). Fifty cells per slide were selected randomly and their olive tail moments were determined using an image analysis system (Komet 3.1, Kinetics Imaging Ltd., Liverpool) linked to a CCD camera.

Measurement of ROS generation. The effects of SeC on intracellular ROS generation were evaluated by DCF fluorescence assay. Briefly, cells were harvested by centrifugation, washed twice with PBS, and suspended in PBS (1×10^6 cells/ml). Cell suspension was incubated with 10 μM DCFH-DA at 37°C for 30 min. After the addition of SeC, the cells were incubated at 37°C for different periods of time and analyzed by flow cytometry.

Caspase activity assay. Harvested cell pellets were suspended in cell lysis buffer and incubated on ice for 1 h. After centrifugation at 11 000 × g for 30 min, supernatants were collected and immediately measured for protein concentration and caspase activity. Briefly, cell lysates were placed in 96-well plates and then specific caspase substrates (Ac-DEVD-AMC for caspase-3, Ac-IETD-AMC for caspase-8 and Ac-LEHD-AMC for caspase-9) were added. Plates were incubated at 37°C for 1 h and caspase activity was determined by fluorescence intensity with the excitation and emission wavelengths set at 380 and 440 nm respectively.

Western blot analysis. Cytosolic extracts were prepared by incubating the cells on ice in hypotonic buffer (20 mM Hepes, 10 mM KCl, 1.5 mM $MgCl_2$, 1 mM EDTA, 1 mM EGTA, 250 mM sucrose, 1 mM dithiothreitol, aprotinin, leupeptin and pepstatin 2 mg/ml each, pH 7.5) for 30 min. Then the cells were disrupted in a Dounce homogenizer by optimal gentle strokes and centrifuged at 1000 g for 10 min at 4°C to remove unbroken cells and nuclei. The homogenates were collected and centrifuged again at 12 000 × g for 30 min at 4°C to separate the mitochondria and cytosol fraction.

Total cellular proteins were extracted by incubating cells in lysis buffer obtained from Cell Signaling Technology. The protein concentrations in the cell lysates were determined by bicinchoninic acid assay (Sigma) according to the manufacturer's instructions. SDS-PAGE was done in 10% tricine gels loading equal amount of proteins per lane. After electrophoresis, separated proteins were transferred to nitrocellulose membrane and blocked with 5% non-fat milk in TBST buffer for 1 h. After that, the membranes were incubated with primary antibodies at 1:1000 dilutions in 5% non-fat milk overnight at 4°C,

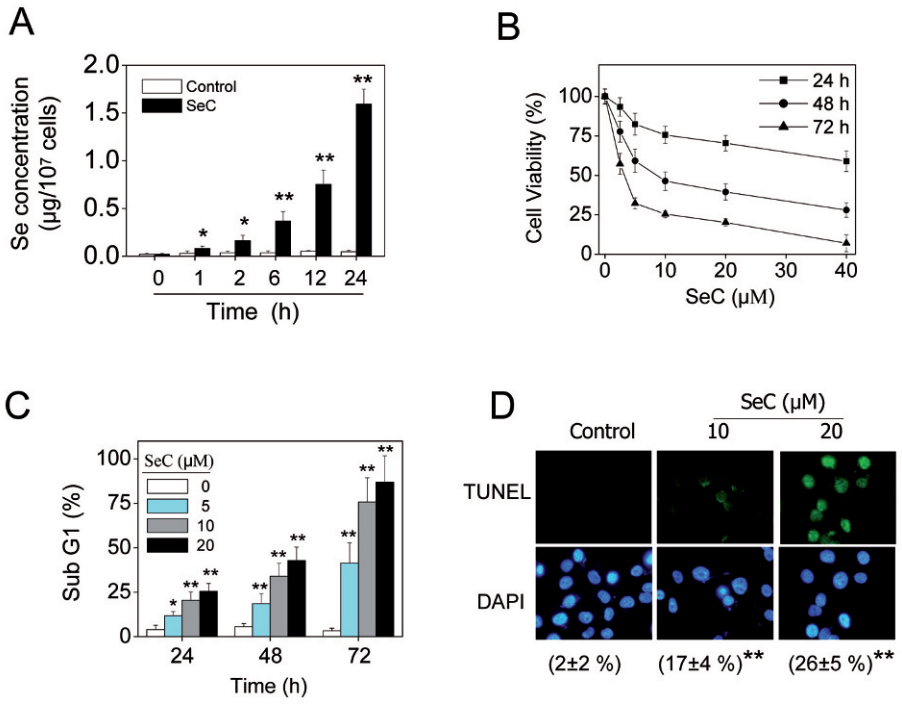

Figure 1. SeC treatment caused cell growth inhibition and apoptosis in A375 cells. (*A*) Quantitative analysis of uptake of Se into cells exposed to 20 μM SeC by ICP-AES analysis. (*B*) Cell viability after treatment with different concentrations of SeC for 24, 48, and 72 h as examined by MTT assay. (*C*) Quantitative analysis of apoptotic cell death induced by SeC by flow cytometric analysis. (*D*) Representative images of DNA fragmentation and nuclear condensation in cells exposed to SeC for 24 h (magnification, 200 x). The apoptotic percentages, as calculated by dividing the TUNEL-positive cell number by the total cell number (DAPI-positive) within the same area, are listed in the parentheses. All results were obtained from three independent experiments. Significant difference between treatment and control groups is indicated at $p<0.05$ (*) or $p<0.01$ (**) level.

and then secondary antibodies conjugated with horseradish peroxidase at 1:2000 dilution for 1 h at room temperature. Protein bands were visualized on X-ray film using an enhanced chemiluminescence system (Kodak). To assess the presence of a comparable amount of proteins in each lane, the membranes were stripped finally to detect the β-actin.

siRNA transfection. Cells were seeded at 2×10^5 cells per well in six-well plates and allowed to grow to 50 % confluence after 24 h. Cells were incubated with 60 nmol/L p53 siRNA and transfection reagent in serum-free culture medium for 24 h, and then 1 ml fresh completed medium was added to each well for another 24 h with or without SeC. Additionally, cells were also transfected with a fluorescein-labeled non-targeted control siRNA, which allows us to monitor the efficiency of transfection. A non-target antibody (p42 MAPK) was used to control for loading and monitor specificity of p53 siRNA.

***in vivo* studies.** Exponentially growing A375 cells (2×10^6) suspended in 200 μl PBS were injected subcutaneously into the right flank of each five-week male nude mouse. Mice were randomized into two groups of 12 mice/group. After one week, SeC dissolved in PBS was given i.p. (10 μg/g body weight per day) for ten days. Control mice received an equal volume of the vehicle (PBS) only. At the termination of the experiments, tumors were excised, photographed, and weighed. A portion of the tumors from control and treated animals was used for preparation of tumor lysate used in further analysis. Tumor dimensions were measured with calipers and the volume was calculated using the formula: volume $= l\times w^2/2$, with l being the maximal length and w being the width. Se content in the tumor tissues was determined by ICP-AES analysis. All animal experiments were approved by the Animal Experimentation Ethics Committee, CUHK.

Statistical analysis. Experiments were carried out at least in triplicate and results were expressed as mean ± SD. Statistical analysis was performed using SPSS statistical package (SPSS 13.0 for Windows; SPSS, Inc. Chicago, IL). Difference between two groups was analyzed by two-tailed Student's t test, and that between three or more groups was analyzed by one-way ANOVA multiple comparisons. Difference with $p<0.05$ (*) or $p<0.01$ (**) was considered statistically significant.

Results

Uptake of SeC and induction of apoptotic cell death in A375 melanoma cells. Firstly, we used the ICP-AES method to investigate the uptake of SeC in A375 cells. As shown in Figure 1A, the intracellular Se concentration increased significantly in a time-dependent manner. Accumulation of SeC in A375 cells resulted in time- and dose-dependent growth inhibition as

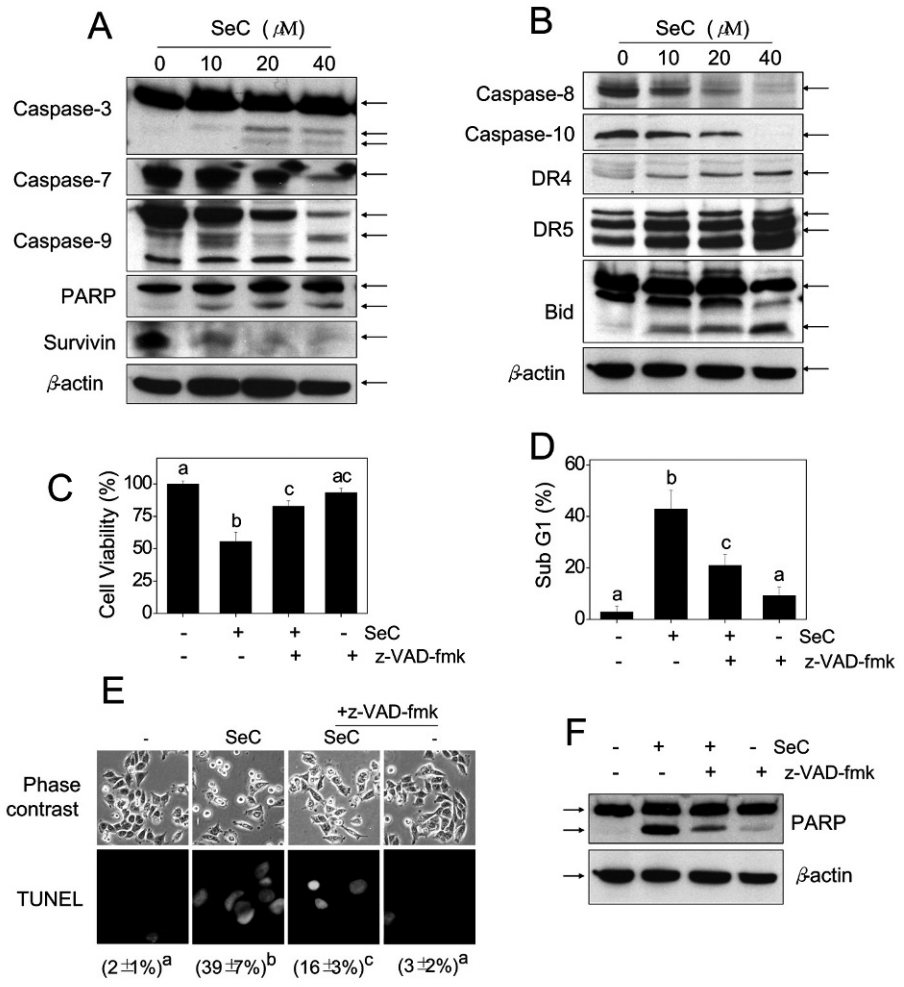

Figure 2. General caspase inhibitor z-VAD-fmk alleviated SeC-induced apoptosis in A375 cells. Cells were pretreated with 60 μM z-VAD-fmk 1 h prior to the treatment of 40 μM SeC for 24 h. (*A* and *B*) Western blot analysis of expression levels of caspase-3, caspase-7, caspase-9, PARP, survivin, caspase-8, caspase-10, DR4, DR5 and Bid. (*C* and *D*) Protective effects of z-VAD-fmk against cell growth inhibition and apoptosis induced by SeC. Apoptotic cell death was analyzed by flow cytometry. (*E*) Changes in cell morphology were examined under light microscopy. Cellular DNA fragmentation was detected by TUNEL assay (magnification, 200 x). The apoptotic percentages, as calculated by dividing the TUNEL-positive cell number by the total cell number are listed below the images. (*F*) Cleavage of PARP was detected by western blotting. All results were obtained from three independent experiments. Values with different characters are statistically different at $p<0.05$ level.

examined by MTT assay (Fig. 1B), with IC_{50} values at 50.1 μM (24 h), 12.8 μM (48 h) and 3.6 μM (72 h) respectively. In contrast, SeC was relatively nontoxic toward HS68 and Detroit 551 human fibroblasts with an IC_{50} values at 432.5 μM and 278.9 μM after a 72 h treatment (data not shown). These results suggest that SeC possesses great selectivity between cancer and normal cells and displays potential application in melanoma chemoprevention. To investigate the kinetics of the apoptotic cell death induced by SeC, we treated the cells with different concentrations of SeC for various times and analyzed the cell cycle distribution by DNA-flow cytometric analysis. Data in Figure 1C showed that SeC induced a dose- and time-dependent increase in the proportion of apoptotic cells as reflected by sub-G1 peak. Apoptotic cell death was further confirmed by DNA fragmentation as examined by TUNEL assay (Fig. 1D).

SeC triggers caspase-dependent apoptosis pathway in A375 cells. Apoptosis can be initiated by two central mechanisms, the extrinsic [5] and intrinsic pathways [4]. To delineate the molecular events initiated by SeC, we first examined the requirement of caspases for the apoptotic program. Exposure of A375 cells to SeC resulted in a dose-dependent activation of caspase-3, caspase-7, caspase-9, caspase-8 and caspase-10 (Figs. 2A and B), which indicated the activation of both the intrinsic and extrinsic apoptosis pathways. Caspase activation subsequently induced proteolytic cleavage of PARP, which serves as a biochemical marker of cells undergoing apoptosis. SeC treatment also strongly decreased the expression level of survivin (Fig. 2A), but did not affect the levels of other IAP (inhibitor of apoptosis protein) family members, including cIAP and XIAP (data not shown). Moreover, increase in expression levels of death receptor DR4 and DR5, and truncation of Bid, a death agonist member of BH3 domain-only protein family, were observed in cells treated with SeC, which confirmed the activation of the extrinsic apoptosis pathway.

To address the significance of caspase activation in SeC-induced apoptosis, we examined the effects of a

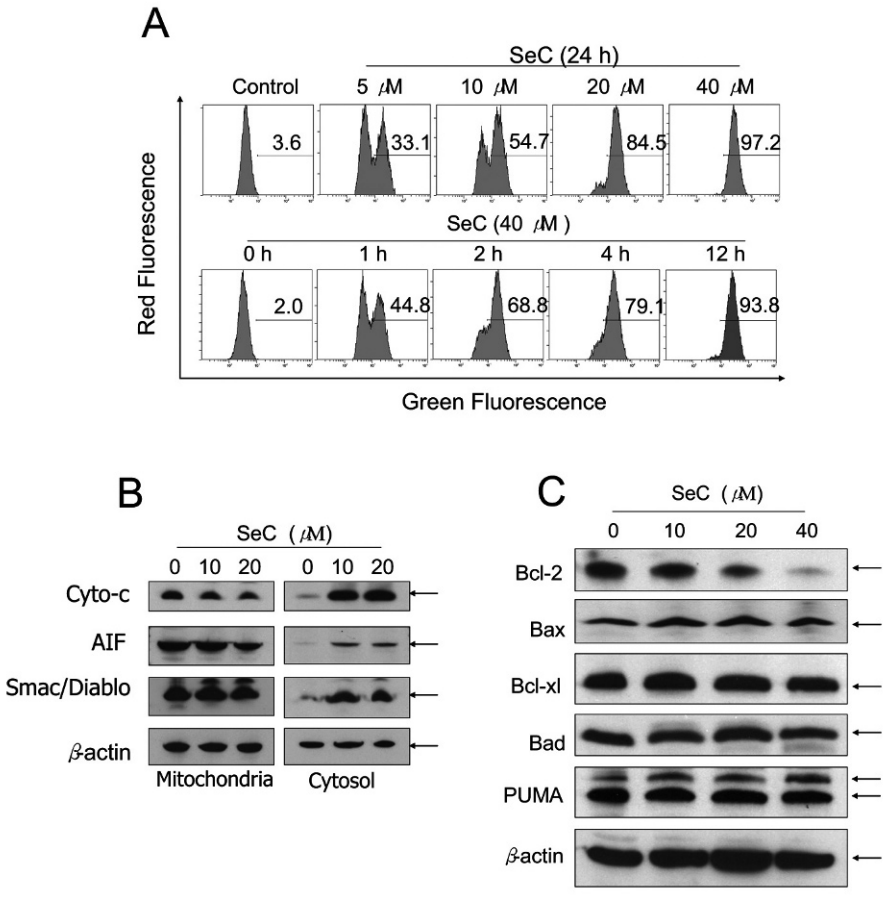

Figure 3. SeC triggered the disruption of mitochondrial membrane potential (MMP), release of apoptogenic factors and alteration in the expression levels of the Bcl-2 family proteins in A375 cells. (*A*) Cells treated with different concentration of SeC for indicated time were stained with JC-1 and then analyzed by flow cytometry. The number presented in each histogram represents the percentage of cells that lost MMP. (*C* and *D*) Western blot analysis of mitochondrial release of cytochrome c (cyto-c), apoptosis-inducing factor (AIF) and Smac/Diablo and the expression levels of Bcl-2, Bax, Bcl-xl, Bad and PUMA in cells treated with indicated concentrations of SeC for 24 h.

general caspase inhibitor z-VAD-fmk. As shown in Figures 2C and D, pretreatment of cells with 60 μM z-VAD-fmk significantly prevented SeC-induced cell death and cell apoptosis as measured by MTT assay and flow cytometric analysis. Consistent with these results, an analysis by microscopy showed that z-VAD-fmk treatment decreased membrane shrinkage, cell rounding, formation of apoptotic bodies and DNA fragmentation induced by SeC (Fig. 2E). The cleavage of PARP was also significantly inhibited by z-VAD-fmk (Fig. 2F), indicating that caspase activity had been effectively abolished. These results indicate that SeC-induced apoptotic cell death occurs mainly in a caspase-dependent manner. However, z-VAD-fmk could not completely prevent PARP cleavage, DNA fragmentation and overall apoptotic cell death, suggesting the existence of a minor component of SeC-induced apoptosis that is independent of caspases.

SeC induces mitochondria dysfunction by regulating the expression of Bcl-2 family proteins. Mitochondria act as a point of integration for apoptotic signals originating from both the extrinsic and intrinsic apoptosis pathways [19]. Loss of mitochondrial membrane potential ($\Delta\Psi m$) is associated with the activation of caspases and the initiation of apoptotic cascades. Therefore, we studied whether SeC-induced apoptosis occurred through destroying mitochondrial homeostasis. A375 cells were treated with different concentrations of SeC for various time and the $\Delta\Psi m$ was assessed by flow cytometry using JC-1 as a molecular probe. JC-1 is a cationic dye that exhibits potential-dependent accumulation in mitochondria. During the loss of $\Delta\Psi m$, the fluorescence of JC-1 dye shifts from red to green. Therefore, the increase in green fluorescence indicates the loss of $\Delta\Psi m$ in the treated cells. As shown in Figure 3A, SeC induced dose- and time- dependent disruption of $\Delta\Psi m$ in A375 cells. A remarkable loss of $\Delta\Psi m$ was observed after 1 h of SeC treatment. Our next task was to determine whether loss of $\Delta\Psi m$ caused a mitochondrial release of apoptogenic factors. As shown in Figure 3B, treatment of SeC dramatically induced the release of cytochrome c, apoptosis-inducing factor (AIF) and Smac/Diablo from mitochondria to the cytosol in a dose-dependent manner.

Bcl-2 family members have been described as key regulators of mitochondrial permeability [20]. Therefore, we examined the effects of SeC on the expression levels of pro-survival and pro-apoptotic Bcl-2 family

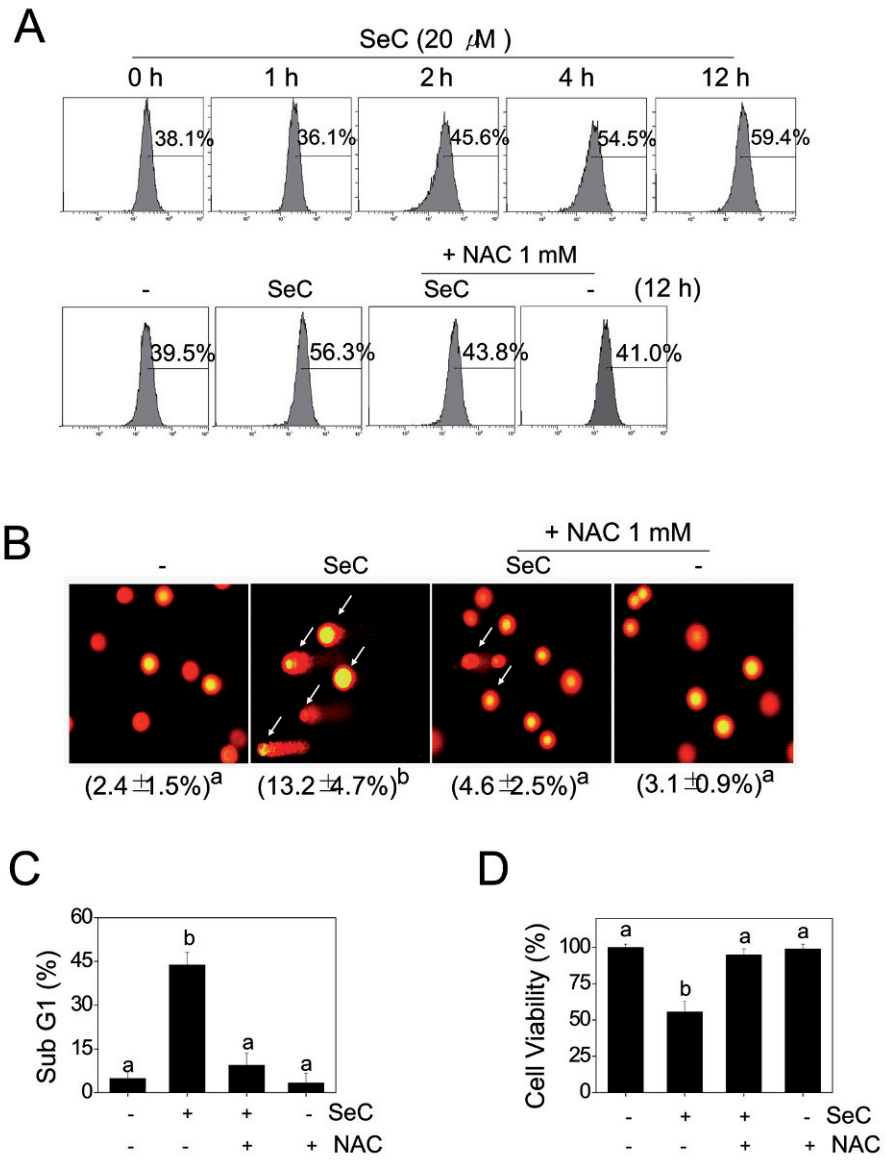

Figure 4. ROS generation and DNA damage were involved in SeC-induced apoptosis in A375 cells. (*A*) Intracellular ROS generation was determined by measuring the fluorescence intensity of an oxidation-sensitive fluorescein DCFH-DA on a flow cytometer. Cells were treated with 20 μM SeC for the indicated time with or without the pretreatment of 1 mM NAC for 4 h. (*B*) Protective effects of NAC on DNA damage induced by SeC. A375 cells were pretreated with NAC (1 mM) for 4 h, followed by incubation with 40 μM SeC for 2 h, and then immediately analyzed by Comet assay as described in section of Materials and methods. Arrow indicates cells with damaged DNA. Average olive tail moment is listed below each image. (*C* and *D*) Protective effects of NAC on cell growth inhibition and apoptosis induced by SeC. A375 cells were pretreated with NAC (1 mM) for 4 h, followed by co-incubation with 40 μM SeC for 24 h, and then immediately subjected to flow cytometric analysis (*C*) and MTT assay (*D*) as described in section of Materials and methods. Values with different characters are statistically different at $p<0.05$ level.

proteins in A375 cells by western blotting. As shown in Figure 3C, SeC significantly suppressed the expression level of Bcl-2, and increased the expression levels of Bax and PUMA-α. In addition, the expression of Bcl-xl, Mcl-1, Bad, Bik and Bok was not affected by SeC treatment (data not shown), thus supporting the specific activation by SeC. The results in Figure 2B demonstrated that SeC induced the truncation of Bid in A375 cells in a dose-dependent manner, which is consistent with the activation of caspase-8 and caspase-10 in response to SeC treatment. These results indicate that mitochondrial-mediated apoptosis in A375 cells triggered by SeC is predominantly associated with down-regulation of Bcl-2/Bax expression ratio and the truncation of Bid.

ROS-mediated DNA damage is involved in SeC-induced apoptosis. It has been reported that ROS play an important role in the induction of apoptosis by various chemopreventive and chemotherapeutic agents [21]. The mitochondrial respiratory chain is a potential source of ROS, such as superoxide and hydrogen peroxide [22]. The observation of mitochondrial dysfunction (Fig. 3) led us to examine the role of ROS in SeC-induced apoptosis. The intracellular ROS generation in A375 cells treated by SeC was measured by DCF-flow cytometry. This assay is based on the cellular uptake of a non-fluorescent probe (DCFH-DA), which is subsequently hydrolyzed by intracellular esterase to form dichlorofluorescin, DCFH. The non-fluorescent substrate is oxi-

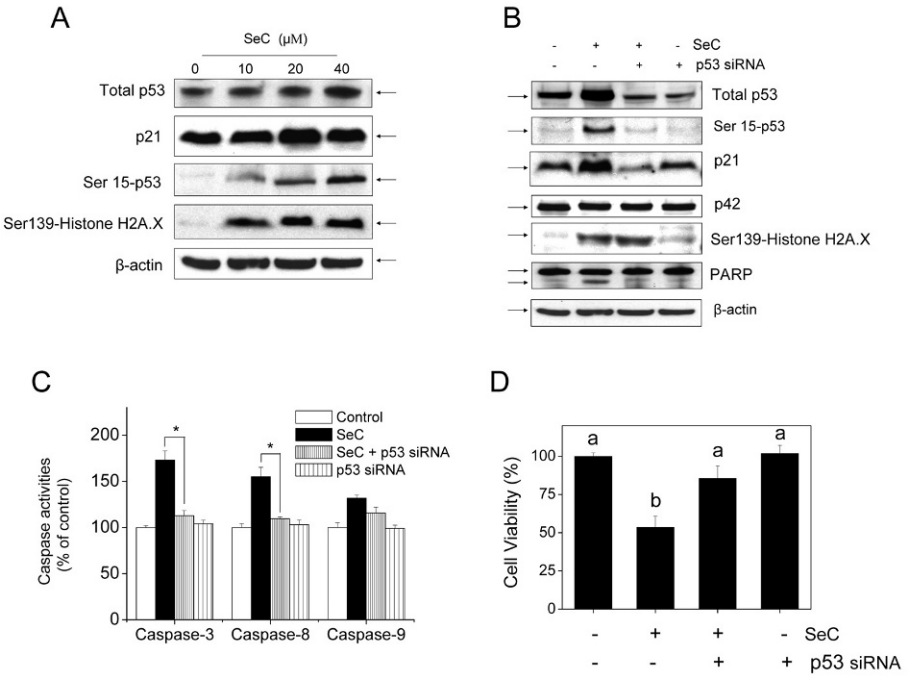

Figure 5. SeC treatment activated p53-dependent apoptosis in A375 cells. (*A*) Western blot analysis of expression levels of p53 and p21Waf1, and phosphorylation of p53 and histone H2A.X in A375 cells exposed to SeC for 24 h. (*B*) Inhibitory effects of p53 siRNA on SeC-induced cell apoptosis, expression and phosphorylation of p53. Cells were transfected with 60 nmol/L of p53 siRNA for 24 h and then treated in combination with SeC for another 24 h. (*C* and *D*) Protective effects of p53 siRNA against caspase activation and cell growth inhibition induced by SeC. Caspase activity was measured using synthetic fluorogenic substrate as described in Materials and methods. Cell viability was examined by MTT assay. Bars with different characters are statistically different at $p<0.05$ level.

dized by the intracellular free radicals, producing a fluorescent product DCF [23]. As shown in Figure 4A, a time-course study showed an increase in ROS generation as early as 2 h after SeC treatment, which peaked at approximately 12 h, followed by a decreasing trend from 12 h to 48 h (data not shown). Pretreatment of the cells with a thiol-reducing antioxidant N-acetylcysteine (NAC) effectively prevented SeC-induced ROS generation (Fig. 4A).

The induction of DNA damage by SeC was investigated by Comet assay, which provides a measure of both single- and double-strand breaks in DNA. Following treatment of SeC, time- and dose-dependent DNA damage was observed in A375 cells (data not shown). As shown in Figure 4B, a significant elevation of DNA strand breaks (DSBs) in A375 cells was detectable in cells exposed to 40 μM SeC for 2 h. Furthermore, we found that SeC-induced DSBs occurred upstream to the caspase activation, because pretreatment of the cells with a general caspase inhibitor z-VAD-fmk showed no protective effects on DNA damage (data not shown).

To further examine the important role of ROS generation in SeC-induced apoptosis, we next investigate the effects of NAC on DSBs and overall apoptotic cell death. Data shown in Figures 4 B and C revealed that 1mM NAC almost completely blocked the increase in Sub-G1 cell populations and DSBs induced by SeC. Thus, SeC-induced cell death was completely suppressed by NAC (Fig. 4D). These results indicate that SeC-induced apoptosis in A375 cells is ROS-dependent.

p53 is a potential target for SeC action in A375 cells. The previous results showed that SeC treatment up-regulated the expression of some p53-inducible genes, such as Bax and PUMA (Fig. 3C), and induced ROS-mediated DNA damage (Fig. 4), suggesting the possible involvement of p53 pathway in SeC-induced apoptosis. To examine whether p53 is activated by SeC, we determined the p53 expression and phosphorylation in A375 cells treated with 10–40 μM SeC for 24 h. As shown in Figure 5A, SeC treatment resulted in elevations of total and phosphorylated p53 at Ser 15 in a dose-dependent manner. However, phosphorylation at residues of Ser6, Ser20, Ser37 and Ser46 was not detected in cells exposed to SeC (data not shown). These results indicated that Ser15 was the major phosphorylation site of p53 induced by SeC. Protein levels of p21Waf1 and a DNA damage marker Ser139-Histone H2A.X were also up-regulated in A375 cells treated with SeC.

The role of p53 in SeC-induced apoptosis pathways was further verified by using RNA interference to reduce the mRNA of this gene. As shown in Figure 5B, transfection of p53 siRNA significantly inhibited the expression levels of total p53, p21Waf1 and phospho-p53 Ser15 in cells treated by SeC, whereas no change in expression level of non-target gene p42 was observed. In contrast, silencing of p53 failed to inhibit the H2A.X phosphorylation in cells exposed to SeC. To further evaluate the requirement for p53 in SeC-induced apoptosis, we next examined the effects of p53 silencing on PARP cleavage, caspase activation and cell viability in cells treated with SeC. The results

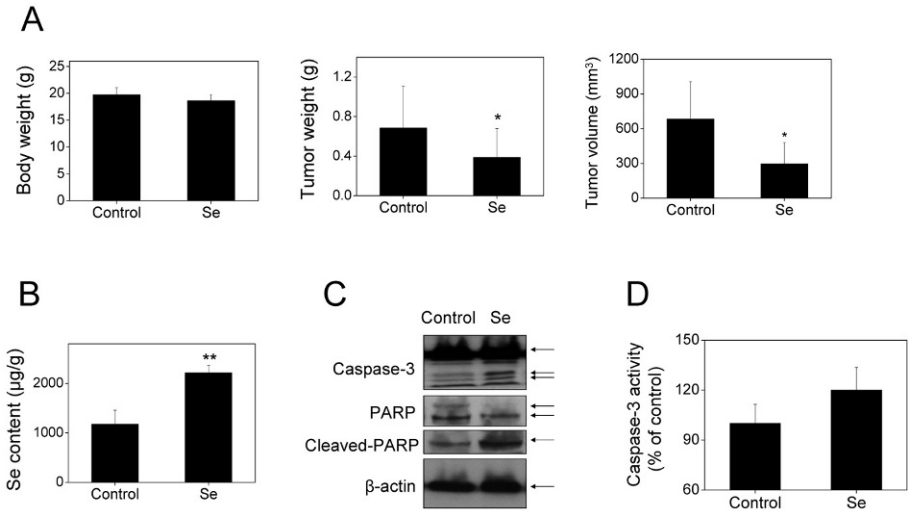

Figure 6. SeC abrogated the growth of melanoma tumor xenografts in nude mice. A375 cells (2×10^6) were injected subcutaneously into five-week male nude mice of twelve per group. After one week, mice were treated i.p. with SeC (10 μg/g body weight per day) for ten days. The control group received vehicle only (PBS). (*A*) Body weight, tumor weight and tumor volume were measured at the end of experiment. (*B*) Se content in the tumors was determined by ICP-MS analysis as described in Materials and methods. (*C* and *D*) Homogenized cell lysates were prepared from the control and SeC-treated tumor tissues from both sets of nude mice. Cleavage of caspase-3 and PARP were examined by western blot analysis. Caspase-3 activity was measured using synthetic fluorogenic substrate (Ac-DEVD-AMC) as described in Materials and methods. Significant difference between treatment and control is indicated at $p<0.05$ (*) or $p<0.01$ (**) level.

indicate that transfection with 60 nM p53 siRNA effectively blocked the SeC-induced PARP cleavage (Fig. 5B), activation of caspase-3, caspase-8 and caspase-9 (Fig. 5C) and growth inhibition (Fig. 5D). In addition, the control siRNA showed no effects on SeC-induced p53 activation and apoptotic cell death (data not shown). Taken together, these results indicate that activation of the p53 pathway is required for SeC-induced apoptosis.

SeC inhibits the growth of A375 xenografts in nude mice through induction of apoptosis. To further examine the therapeutic effect of SeC *in vivo*, we treated immuno-deficient nude mice bearing A375 tumor xenografts with 10 mg/kg/day of SeC for ten days. At the end of the experiments, body weight, tumor weight, tumor volume and total Se concentration in the tumor were measured. As shown in Figure 6A, the tumor weight and tumor volume of the SeC-treated group were significantly reduced in comparison to those of the vehicle treated control group. Furthermore, no significant difference in body weight of animals was observed between the control and treatment groups. These results suggest that SeC not only inhibits human melanoma cell proliferation *in vitro* but also has therapeutic activity *in vivo*.

Our previous results in cell models demonstrated that SeC induced caspase-dependent apoptosis in A375 cells, therefore we evaluated the uptake of SeC and the induction of apoptosis in A375 tumor xenografts. As shown in Figure 6B, treatment with SeC significantly increased the total Se concentration in the tumors from 1178.9 μg/g (control group) to 2214.8 μg/g (treatment group). Accumulation of SeC resulted in the cleavage of caspase-3 and PARP (Fig. 6C). Consistent with the results of western blotting, an increase in caspase-3 activity was observed in A375 tumors exposed to SeC (Fig. 6D). These findings indicate that growth inhibition of A375 tumor xenografts by SeC is due to induction of apoptosis with involvement of caspase activation.

Discussion

Resistance of malignant melanoma cells to drug-induced apoptosis is now recognized as an important mechanism for melanoma malignancy. Therefore, new effective apoptosis-inducing agents with less non-specific toxic effects are currently being intensively searched for. In this study, we demonstrated that SeC, naturally occurring selenoamino acid, showed *in vitro* and *in vivo* inhibitory effects on A375 melanoma cells through induction of apoptosis. Results of mechanistic studies indicated that SeC induced apoptosis of A375 cells by activating ROS-mediated mitochondrial pathway and p53 phosphorylation.

Apoptosis is a critical cellular event for cancer chemoprevention and chemotherapy mediated by selenocompound [11]. Caspases, a family of cysteine acid proteases, are known to act as important mediators of apoptosis induced by different stimuli and

contribute to the overall apoptotic morphology by cleavage of various cellular substrates [24]. Our data showed that SeC induced apoptosis of A375 cells as judged by cell morphology, DNA fragmentation, multiple caspase activation and PARP cleavage (Fig. 1). Cleavage of caspase-8/-10 and caspase-9 suggests the activation of both extrinsic and intrinsic apoptosis pathways, which was further confirmed by the up-regulation of death receptor expression and the mitochondrial dysfunction. The extrinsic pathway was also found to crosstalk with the intrinsic pathway through the truncation of Bid, which relayed the apoptotic signal from the cell surface to mitochondria. Treatment with SeC resulted in an extremely sharp decrease in expression level of survivin, a member of the IAP family [25], which might contribute to the observed activation of caspase-3, caspase-7 and caspase-9. Moreover, we provided convincing evidence that the SeC-induced apoptosis is predominantly executed through activation of caspases. However, the failure of the general caspase inhibitor z-VAD-fmk to completely suppress overall apoptosis induced by SeC suggests the existence of a minor caspase-independent apoptosis pathway.

Mitochondria act as a point of integration for apoptotic signals because both the intrinsic and extrinsic pathways can converge at the mitochondrial level and trigger mitochondrial membrane permeabilization [26]. Disruption of $\Delta\Psi m$ leads to the redistribution of apoptogenic factors, such as cytochrome c, apoptosis-inducing factor (AIF), SMAC/Diablo and endonuclease G [19]. In the present study, A375 cells showed rapid depletion of $\Delta\Psi m$ as early as 1 h following exposure to SeC, and it reached a plateau within 12 h. These results are consistent with the hypothesis that the loss of $\Delta\Psi m$ is an early cellular event in mitochondria-mediated apoptosis [26]. Mitochondrial release of cytochrome c, AIF and SMAC/Diablo was also observed in A375 cells treated with SeC. Released cytochrome c would form an apoptosome with apoptosis activating factor 1 (Apaf-1) and caspase-9, and subsequently activate caspase-mediated apoptosis pathway [4, 6]. Smac/Diablo in the cytosol could bind to IAP family members and promote cytochrome c-mediated caspase activation [27, 28]. Moreover, AIF in the cytosol would translocate into the nucleus where AIF causes large-scale DNA fragmentation and results in caspase-independent apoptosis [29, 30].

The mitochondrial apoptosis pathway is tightly regulated by Bcl-2 family proteins that comprise both pro-apoptotic proteins, such as Bax, Bad and Bid, and anti-apoptotic proteins, such as Bcl-2 and Bcl-xL. Bcl-2 and Bcl-xL bind to the outer membrane of mitochondria and block cytochrome c efflux. However, upon apoptotic stimulation, Bax specifically translocates to the mitochondria membrane and forms membrane-integrated homo-oligomers with Bak, which permeabilize the outer mitochondrial membrane and trigger the loss of $\Delta\Psi m$ followed by the release of apoptogenic factors into cytoplasm [20]. Not surprisingly, many anticancer drugs trigger mitochondria-mediated apoptosis in cancer cells through down-regulation of Bcl-2/Bcl-xL and/or up-regulation of Bax/Bad/Bid. Resistance of melanoma cells to drug-induced apoptosis has been correlated with a defect in cytochrome c release [31] and with the expression levels of anti-apoptotic Bcl-2 family members [32]. Our results show that SeC treatment significantly down-regulated Bcl-2 expression but slightly up-regulated Bax and PUMA-α expression. Thus, down-regulation of the Bcl-2/Bax expression ratio could be a predominant mechanism by which SeC induces mitochondria-mediated apoptosis in A375 cells. In addition, truncation of Bid was also observed in cells exposed to SeC, which could be the result of the activation of the extrinsic apoptosis pathway. Truncated Bid could induce oligomerization of Bak and Bax, thereby promoting the release of mitochondrial proteins into cytoplasm.

Due to the reactive nature of ROS, overproduction of ROS in the cells often results in the accumulation of oxidative products of DNA, proteins, and lipids. Growing evidence suggests that ROS is a key mediator of cell apoptosis induced by Se compounds [12, 33, 34]. ROS-mediated apoptosis was thought to be associated with the dysfunction of the mitochondrial respiratory chain and redistribution of cytochrome c, as well as alteration in mitochondrial membrane permeability [35]. Results from Figure 4A indicate that A375 cells showed rapid intracellular oxidation as early as 2 h following exposure to SeC, which peaked at approximately 12 h and decreased afterward. ROS can be produced from various intracellular sources, such as mitochondrial respiration, xanthine oxidase and NADPH oxidase [36]. In most of the mammalian cell types, mitochondria represent a potential source for ROS generation [37]. In the present study, we found that allopurinol and diphenyleneiodonium chloride, the specific inhibitors of xanthine oxidase and NADPH oxidase, showed little inhibition on SeC-induced ROS generation in A375 cells (data not shown). In addition, rapid disruption of $\Delta\Psi m$ after SeC treatment was detected in A375 cells by JC-1 flow cytometric analysis. These results suggest the involvement and important role of mitochondria in SeC-induced ROS generation. Furthermore, it was also found that NAC, a precursor of glutathione, effectively reduced ROS production and apoptotic cell death in SeC-treated cells. NAC have been reported to act not only as free radical scavengers, but also by replenish-

ing intracellular stores of endogenous antioxidants, or as thiol-reducing agents [38]. Our results suggest the possibility that SeC oxidized intracellular thiol-containing reducing agents like GSH and thioredoxin, and thereby allowed the accumulation of ROS, which led to redox modulation, oxidative DNA damage and cell apoptosis. This is consistent with a previous study which showed that selenite and SeC generated superoxide anion by oxidation of glutathione and other protein thiols in the human mammary tumor cells [39]. Another comparable mechanistic investigation by Kim et al. [40] showed that selenite, SeC, and selenodioxide induced apoptosis in HepG2 cells and oxidizing protein thiols in both HepG2 cells and isolated mitochondria. Therefore, the results from our studies and others suggest that the pro-apoptotic action of SeC is mediated by both thiol group oxidation and the generation of ROS, both of which contribute to opening of the mitochondrial permeability transition (MPT) pore and mitochondrial release of apoptogenic factors.

Excessive production of ROS may inflict damage to various cellular components such as DNA and protein, which leads to the generation of a variety of ROS-mediated modified products like oxidized bases, DNA strand breaks and DNA–protein crosslinks [41]. DNA damage has been reported to be involved in chemopreventive action of some selenocompounds [42]. For instance, Zhou et al. [43] found that selenite, a highly oxidized inorganic Se species, induced chromosomal DSBs and subsequently triggered cell apoptosis by activating ATM/ATR and TOP II pathways. In the present study, SeC treatment induced time- and dose-dependent DSBs in A375 cells. It was also found that SeC-induced DSBs occurred downstream to ROS generation and upstream to the caspase activation, because this damage was almost completely suppressed by an ROS scavenger NAC but not by the general caspase inhibitor z-VAD-fmk. To clarify the role of ROS in the action mechanisms of SeC, we evaluated the effects of NAC on SeC-induced apoptosis. The results showed that pretreatment of NAC significantly suppressed the SeC-induced ROS generation and DSBs in A375 cells (Figs. 4 A and B). NAC treatment also prevented the SeC-induced apoptotic cell death as evidenced by decrease in Sub-G1 cell population and increase in cell viability (Figs. 4 C and D). These results suggest that SeC-induced apoptosis in A375 cells is ROS-dependent.

DSB is one of the most dangerous types of DNA damage that occurs within the cells [44]. A very early cellular event induced by DSB is the phosphorylation of a histone H2A variant, H2A.X, at the sites of DNA damage [45]. For instance, H2A.X was rapidly phosphorylated (within seconds) at serine 139 when DSBs are introduced into mammalian cells [46]. Thus, we analyzed the phosphorylation of histone H2A.X on serine 139 by western blotting. As shown in Figure 5A, a significant increase in this phosphorylated protein was observed in A375 cells treated with 10–40 μM SeC. This result suggests that a DNA damage-mediated pathway is involved in cell apoptosis induced by SeC.

Accumulative evidence suggested that DNA damage caused apoptotic cell death via various signaling pathways [47]. p53 is a transcription factor which can directly or indirectly induce cell apoptosis through both the extrinsic and intrinsic apoptosis pathways [48]. DNA damage can activate the p53 pathway by activating various damage sensor proteins such as ATM (ataxia telangiectasia mutated), ATR (ataxia telangiectasia and Rad3-related) and DNA-PK (DNA-dependent protein kinase), and protein kinases such as Chk1 and Chk2 [47, 49]. We have demonstrated that p53 activation and phosphorylation were required for SeC-induced apoptosis in A375 cells. As shown in Figure 5A, protein levels of total p53 and Ser 15-p53 and its target gene p21Waf1 were upregulated by SeC treatment. Meanwhile, phosphorylation of H2A.X in cells exposed to SeC suggests that DNA damage may be the underlying mechanism that activated the p53 pathway. However, these effects of SeC were completely blocked by pretreatment with NAC. These results indicate that treatment with SeC produces ROS-mediated DNA damage and subsequently activates p53 phosphorylation, suggesting that ROS may be an upstream mediator for p53 activation in A375 cells. The importance of p53 in SeC-induced apoptosis in A375 cells was further demonstrated by the introduction of p53 siRNA. The results showed that silencing of p53 effectively down-regulated the expression levels of total p53, Ser 15-p53 and p21Waf1, and decreased the SeC-induced mitochondrial dysfunction and caspase activation. Furthermore, examination of cell viability showed that silencing of p53 rescued A375 cells from SeC-induced growth inhibition. These results suggest that mitochondria-mediated apoptosis triggered by SeC in A375 cells is p53 dependent. Additionally, the failure of p53 siRNA to inhibit the H2A.X phosphorylation induced by SeC indicated that ROS-mediated DNA damage may be an upstream mediator for p53 phosphorylation and activation.

p53 induces apoptosis by target gene regulation and transcription-independent signaling [50]. In transcription-dependent pathway, p53 activates a number of downstream genes that function in cellular responses to stimuli, including pro-apoptotic genes like Noxa and Puma, Bax, p53 AIP1 and Apaf-1, and pro-survival genes like Bcl-2 and Bcl-xL [51]. In the

transcription-independent pathway, mitochondrial p53 localization directly induces mitochondrial permeabilization, cytochrome c release and caspase activation by forming complexes with mitochondrial pro-survival proteins such as p53AIP1 and Bcl-2/Bcl-xL [52, 53]. Our results demonstrated that SeC significantly down-regulated the expression level of Bcl-2, and slightly increased the expression levels of Bax and PUMA-α. However, no mitochondrial translocation of p53 was observed in A375 cells treated with SeC as examined by western blot analysis and immunofluorescence staining. Therefore, we conclude that p53 induces mitochondria-mediated apoptosis in A375 cells in response to SeC treatment through transcription-dependent pathway.

In summary, our results suggest that SeC inhibits the growth of human melanoma cells *in vivo* and *in vitro* through induction of caspase-mediated apoptosis. Investigation on the molecular mechanisms demonstrates that apoptosis triggered by SeC is ROS mediated and p53-dependent via mitochondrial pathways. ROS acts as an upstream mediator for p53 activation. On the other hand, p53 activation synergistically enhances ROS generation through induction of mitochondrial dysfunction. Based on these results, we suggest that SeC may be a candidate for further evaluation as a chemopreventive agent for human cancer, especially melanoma cancers.

Acknowledgements. This work was supported by the Food Science Research Fund of The Chinese University of Hong Kong (6901999) and the Institute of Plant Molecular Biology and Agricultural Biotechnology Research Fund (1901037).

1 Rigel, D. S. and Carucci, J. A. (2000). Malignant melanoma: prevention, early detection, and treatment in the 21st century. CA Cancer J Clin 50, 215–36; quiz 237–40.
2 Chin, L., Garraway, L. A. and Fisher, D. E. (2006). Malignant melanoma: genetics and therapeutics in the genomic era. Genes Dev 20, 2149–82.
3 de Vries, E., Bray, F. I., Coebergh, J. W. and Parkin, D. M. (2003). Changing epidemiology of malignant cutaneous melanoma in Europe 1953–1997: rising trends in incidence and mortality but recent stabilizations in western Europe and decreases in Scandinavia. Int J Cancer 107, 119–26.
4 Li, P., Nijhawan, D., Budihardjo, I., Srinivasula, S. M., Ahmad, M., Alnemri, E.S. and Wang, X. (1997). Cytochrome c and dATP-dependent formation of Apaf-1/caspase-9 complex initiates an apoptotic protease cascade. Cell 91, 479–89.
5 Nagata, S. (1997). Apoptosis by death factor. Cell 88, 355–65.
6 Kim, R. (2005). Recent advances in understanding the cell death pathways activated by anticancer therapy. Cancer 103, 1551–60.
7 Zapata, J. M., Pawlowski, K., Haas, E., Ware, C. F., Godzik, A. and Reed, J. C. (2001). A diverse family of proteins containing tumor necrosis factor receptor-associated factor domains. J Biol Chem 276, 24242–52.
8 Ivanov, V. N., Bhoumik, A. and Ronai, Z. (2003). Death receptors and melanoma resistance to apoptosis. Oncogene 22, 3152–61.
9 Schomburg, L., Schweizer, U. and Kohrle, J. (2004). Selenium and selenoproteins in mammals: extraordinary, essential, enigmatic. Cell Mol Life Sci 61, 1988–95.
10 Schrauzer, G. N. (2000). Anticarcinogenic effects of selenium. Cell Mol Life Sci 57, 1864–73.
11 Sinha, R. and El-Bayoumy, K. (2004). Apoptosis is a critical cellular event in cancer chemoprevention and chemotherapy by selenium compounds. Curr Cancer Drug Targets 4, 13–28.
12 Zhao, R., Xiang, N., Domann, F. E. and Zhong, W. (2006). Expression of p53 enhances selenite-induced superoxide production and apoptosis in human prostate cancer cells. Cancer Res 66, 2296–304.
13 Li, D., Graef, G. L., Yee, J. A. and Yan, L. (2004). Dietary supplementation with high-selenium soy protein reduces pulmonary metastasis of melanoma cells in mice. J Nutr 134, 1536–40.
14 Yan, L., Yee, J. A., Li, D., McGuire, M. H. and Graef, G. L. (1999). Dietary supplementation of selenomethionine reduces metastasis of melanoma cells in mice. Anticancer Res 19, 1337–42.
15 Traynor, N. J., McKenzie, R. C., Beckett, G. J. and Gibbs, N. K. (2006). Selenomethionine inhibits ultraviolet radiation-induced p53 transactivation. Photodermatol Photoimmunol Photomed 22, 297–303.
16 Chen, T. and Wong, Y. S. (in press). Selenocystine induces reactive oxygen species-mediated apoptosis in human cancer cells. Biomed Pharmacother
17 Chen, T., Wong, Y. S. and Zheng, W. (2006). Purification and characterization of selenium-containing phycocyanin from selenium-enriched Spirulina platensis. Phytochemistry 67, 2424–30.
18 Chen, T., Zheng, W., Wong, Y. S. and Yang, F. (2008). Mitochondria-mediated apoptosis in human breast carcinoma MCF-7 cells induced by a novel selenadiazole derivative. Biomed Pharmacother 62, 77–84.
19 van Gurp, M., Festjens, N., van Loo, G., Saelens, X. and Vandenabeele, P. (2003). Mitochondrial intermembrane proteins in cell death. Biochem Biophys Res Commun 304, 487–97.
20 Cory, S. and Adams, J. M. (2002). The Bcl2 family: regulators of the cellular life-or-death switch. Nat. Rev. Cancer 2, 647–56.
21 Pelicano, H., Carney, D. and Huang, P. (2004). ROS stress in cancer cells and therapeutic implications. Drug Resist Updat 7, 97–110.
22 Turrens, J. F. (2003). Mitochondrial formation of reactive oxygen species. J Physiol 552, 335–44.
23 LeBel, C. P., Ischiropoulos, H. and Bondy, S. C. (1992). Evaluation of the probe 2',7'-dichlorofluorescin as an indicator of reactive oxygen species formation and oxidative stress. Chem Res Toxicol 5, 227–31.
24 Riedl, S. J. and Shi, Y. (2004). Molecular mechanisms of caspase regulation during apoptosis. Nat Rev Mol Cell Biol 5, 897–907.
25 Deveraux, Q. L. and Reed, J. C. (1999). IAP family proteins—suppressors of apoptosis. Genes Dev 13, 239–52.
26 Henry-Mowatt, J., Dive, C., Martinou, J. C. and James, D. (2004). Role of mitochondrial membrane permeabilization in apoptosis and cancer. Oncogene 23, 2850–60.
27 Du, C., Fang, M., Li, Y., Li, L. and Wang, X. (2000). Smac, a mitochondrial protein that promotes cytochrome c-dependent caspase activation by eliminating IAP inhibition. Cell 102, 33–42.
28 Srinivasula, S. M., Hegde, R., Saleh, A., Datta, P., Shiozaki, E., Chai, J., Lee, R. A., Robbins, P. D., Fernandes-Alnemri, T., Shi, Y. and Alnemri, E. S. (2001). A conserved XIAP-interaction motif in caspase-9 and Smac/DIABLO regulates caspase activity and apoptosis. Nature 410, 112–6.
29 Krantic, S., Mechawar, N., Reix, S. and Quirion, R. (2007). Apoptosis-inducing factor: a matter of neuron life and death. Prog Neurobiol 81, 179–96.
30 Modjtahedi, N., Giordanetto, F., Madeo, F. and Kroemer, G. (2006). Apoptosis-inducing factor: vital and lethal. Trends Cell Biol 16, 264–72.

31 Raisova, M., Bektas, M., Wieder, T., Daniel, P., Eberle, J., Orfanos, C. E. and Geilen, C.C. (2000). Resistance to CD95/Fas-induced and ceramide-mediated apoptosis of human melanoma cells is caused by a defective mitochondrial cytochrome c release. FEBS Lett 473, 27–32.
32 Fecker, L. F., Geilen, C. C., Tchernev, G., Trefzer, U., Assaf, C., Kurbanov, B.M., Schwarz, C., Daniel, P. T. and Eberle, J. (2006). Loss of proapoptotic Bcl-2-related multidomain proteins in primary melanomas is associated with poor prognosis. J Invest Dermatol 126, 1366–71.
33 Jung, U., Zheng, X., Yoon, S. O. and Chung, A. S. (2001). Se-methylselenocysteine induces apoptosis mediated by reactive oxygen species in HL-60 cells. Free Radic Biol Med 31, 479–89.
34 Nilsonne, G., Sun, X., Nystrom, C., Rundlof, A. K., Potamitou Fernandes, A., Bjornstedt, M. and Dobra, K. (2006). Selenite induces apoptosis in sarcomatoid malignant mesothelioma cells through oxidative stress. Free Radic Biol Med 41, 874–85.
35 Boya, P., Morales, M. C., Gonzalez-Polo, R. A., Andreau, K., Gourdier, I., Perfettini, J. L., Larochette, N., Deniaud, A., Baran-Marszak, F., Fagard, R., Feuillard, J., Asumendi, A., Raphael, M., Pau, B., Brenner, C. and Kroemer, G. (2003). The chemopreventive agent N-(4-hydroxyphenyl)retinamide induces apoptosis through a mitochondrial pathway regulated by proteins from the Bcl-2 family. Oncogene 22, 6220–30.
36 Valko, M., Rhodes, C. J., Moncol, J., Izakovic, M. and Mazur, M. (2006). Free radicals, metals and antioxidants in oxidative stress-induced cancer. Chem Biol Interact 160, 1–40.
37 Gonzalez, C., Agapito, M. T., Rocher, A., Gonzalez-Martin, M. C., Vega-Agapito, V., Gomez-Nino, A., Rigual, R., Castaneda, J. and Obeso, A. (2007). Chemoreception in the context of the general biology of ROS. Respir Physiol Neurobiol 157, 30–44.
38 Valko, M., Leibfritz, D., Moncol, J., Cronin, M. T., Mazur, M. and Telser, J. (2007). Free radicals and antioxidants in normal physiological functions and human disease. Int J Biochem Cell Biol 39, 44–84.
39 Yan, L. and Spallholz, J. E. (1993). Generation of reactive oxygen species from the reaction of selenium compounds with thiols and mammary tumor cells. Biochem Pharmacol 45, 429–37.
40 Kim, T. S., Yun, B. Y. and Kim, I. Y. (2003). Induction of the mitochondrial permeability transition by selenium compounds mediated by oxidation of the protein thiol groups and generation of the superoxide. Biochem Pharmacol 66, 2301–11.
41 Lloyd, D. R., Phillips, D. H. and Carmichael, P. L. (1997). Generation of putative intrastrand cross-links and strand breaks in DNA by transition metal ion-mediated oxygen radical attack. Chem Res Toxicol 10, 393–400.
42 Letavayova, L., Vlckova, V. and Brozmanova, J. (2006). Selenium: from cancer prevention to DNA damage. Toxicology 227, 1–14.
43 Zhou, N., Xiao, H., Li, T. K., Nur, E. K. A. and Liu, L. F. (2003). DNA damage-mediated apoptosis induced by selenium compounds. J Biol Chem 278, 29532–7.
44 Modesti, M. and Kanaar, R. (2001). DNA repair: spot(light)s on chromatin. Curr Biol 11, R229–32.
45 Burma, S., Chen, B. P., Murphy, M., Kurimasa, A. and Chen, D. J. (2001). ATM phosphorylates histone H2AX in response to DNA double-strand breaks. J Biol Chem 276, 42462–7.
46 Rogakou, E. P., Pilch, D. R., Orr, A. H., Ivanova, V. S. and Bonner, W. M. (1998). DNA double-stranded breaks induce histone H2AX phosphorylation on serine 139. J Biol Chem 273, 5858–68.
47 Roos, W. P. and Kaina, B. (2006). DNA damage-induced cell death by apoptosis. Trends Mol Med 12, 440–50.
48 Hofseth, L. J., Hussain, S. P. and Harris, C.C. (2004). p53: 25 years after its discovery. Trends Pharmacol Sci 25, 177–81.
49 Sancar, A., Lindsey-Boltz, L. A., Unsal-Kacmaz, K. and Linn, S. (2004). Molecular mechanisms of mammalian DNA repair and the DNA damage checkpoints. Annu Rev Biochem 73, 39–85.
50 Mihara, M., Erster, S., Zaika, A., Petrenko, O., Chittenden, T., Pancoska, P. and Moll, U. M. (2003). p53 has a direct apoptogenic role at the mitochondria. Mol Cell 11, 577–90.
51 Vousden, K. H. and Lu, X. (2002). Live or let die: the cell's response to p53. Nat Rev Cancer 2, 594–604.
52 Marchenko, N. D., Zaika, A. and Moll, U. M. (2000). Death signal-induced localization of p53 protein to mitochondria. A potential role in apoptotic signaling. J Biol Chem 275, 16202–12.
53 Zhao, Y., Chaiswing, L., Velez, J. M., Batinic-Haberle, I., Colburn, N.H., Oberley, T.D. and St Clair, D.K. (2005). p53 translocation to mitochondria precedes its nuclear translocation and targets mitochondrial oxidative defense protein-manganese superoxide dismutase. Cancer Res 65, 3745–50.